# Detection of Moving Targets in Automotive Radar with Distorted Ego-Velocity Information

Christopher Grimm, Ridha Farhoud, Tai Fei, Ernst Warsitz
Hella KGaA Hueck & Co
59555 Lippstadt, Germany
Email: {christopher.grimm, ridha.farhoud, tai.fei, ernst.warsitz}@hella.com

Reinhold Haeb-Umbach
Department of Communication Engineering
University of Paderborn
33098 Paderborn, Germany
Email: haeb@nt.uni-paderborn.de

***Abstract*—In this paper we present an algorithm for the detection of moving targets in sight of an automotive radar sensor which can handle distorted ego-velocity information. In situations where biased or none velocity information is provided from the ego-vehicle, the algorithm is able to estimate the ego-velocity based on previously detected stationary targets with high accuracy, subsequently used for the target classification. Compared to existing ego-velocity algorithms our approach provides fast and efficient inference without sacrificing the practical classification accuracy. Other than that the algorithm is characterized by simple parameterization and little but appropriate model assumptions for high accurate production automotive radar sensors.**

***Keywords*—radar, relocity, classification**

## I. Introduction

In order to provide driver assistance functionality like Adaptive Cruise Control (ACC), Rear Cross Traffic Alert (RCTA) and Blindspot Detection, more and more cars are equipped with Radar sensors as a distance, relative velocity and angle measurement equipment for objects in the vehicles environment. From these measurements a understanding of the complex vehicles surrounding is generated via classification algorithms which discriminate the detected radar targets into different object classes with certain behaviors of interest. One very basic discrimination lies in the separation of stationary and dynamic targets, since the latter one can change their relative position to the ego-vehicle they certainly require more sophisticated tracking and control actions than the former one. After this initial classification, a subsequently and more complex classification of dynamic targets could be performed to provide even better scene understanding. However in this paper we focus on the pure discrimination between dynamic and stationary targets.

This task has already seen some treatment by [1], [2], [3], [4], [5], [6], where most of the publcations focus on the detection of stationary targets in order to estimate the ego-vehicles states of motion or estimating a correction model for the angle of arrival based on stationary targets. The proposed classifiers from these literature have in common, that a good ego-velocity (longitudinal velocity) knowledge significantly influences the performance of the classifier itself, since they all share the same functional relationship between stationary targets and the relative moving vehicle, which will be presented later. In the papers [1], [2], [3] the authors utilize once detected stationary targets to provide precise estimate of the ego motion. As a classifier a RANSAC algorithm was performed to extract a major group of targets and assign them to be stationary, which we did not found to pay adequate attention to specific radar properties, like uncertainties of different measurements. Also the iterative and costly RANSAC disqualifies the algortihm for the usage on low performant embedded hardware which is used for series production radar sensors. In [4] the author expects a stationary border parallel to the ego-vehicle and then estimating an adaptive correction model for the angle of targets as well as the ego-velocity. As long as a stationary border is detected, the velocity estimation will help to improve the classifier, but since this can not be guaranteed for the general driving situation, this assumption introduces significant drawback. In [6] the authors provide a fast and easy to compute classification algorithm which respects the radar specific uncertainties. However, it is feed by velocity estimations via the vehicles wheel encoders which measure the revs of the wheels. Under the assumption of neglecting tire slip and with the knowledge of the tire diameter, it is possible to estimate the ego-velocity sufficiently well. However, this so called odometric velocity estimation has significant drawbacks. For example, if the tire diameter is not known exactly, the estimation will result in velocity proportional error. Also the odometric sensors need a minimum angular wheel velocity to provide reliable velocity estimate, resulting in a non observable velocity estimate at low vehicle velocities. These inaccuracies in velocity can be seen in Figure 6.

In this paper we adapt the propsed classifier from [6] and extend it with a radar based vehicle velocity estimator in order to improve accuracy and robustness of classification. In contrast to the other algorithms, the proposed algorithm features capability for operating in arbitrary environment situations as well as a strictly feed forward inference.

## II. Ego-Velocity Estimation

### A. Statistical Framework for Stationary Target Detection

We utilize the statistical hypothesis test presented in [6] for the detection of stationary radar targets. In this approach, the likelihood for a stationary target is calculated from the ego-velocity, which is provided by the vehicle manufacturer via the vehicles CAN-Bus, the radar measured azimuth angle

978-1-5090-5391-9/17/$31.00  

of the incoming reflecting target and the relative speed of the target. Since the variables are modeled as random variables, an confidence interval of the difference $e$ between the measured and the expected velocity of the raw targets is calculated. If the difference between the measured velocity and the expectation lies outside the parametrized interval for stationary raw targets $\left(\mu_E \pm \sigma_E \cdot Q^{-1}(\alpha/2)\right)$, then it is not probable that it stems from a stationary target, described by $H_0$ Hypothesis

$$\begin{aligned} \text{reject } H_0, \text{ if } e &\leq \mu_E - \sigma_E \cdot Q^{-1}(\alpha/2) \\ \text{or } e &\geq \mu_E + \sigma_E \cdot Q^{-1}(\alpha/2). \end{aligned} \tag{1}$$

The equation is characterized by a deterministic velocity difference $\mu_E$ and expected velocity standard deviation $\sigma_E$ due to uncertainties in measurements. The term $Q$ scales the uncertainty with respect to the desired significance level $\alpha$. Further factors of influence for the interval are the angle of incidence $\hat{\mu}_\Phi$ of a reflecting target and the ego-velocity $\mu_{V_{\text{Ego}}}$. Likewise, the standard deviation of the ego-velocity measurement $\sigma_{V_{\text{Ego}}}$, the standard deviation of the angle measurement $\hat{\sigma}_\Phi$ and the standard deviation of the relative velocity measurement by radar $\sigma_{v_r}$ have considerable influence.

As mentioned before, for the best classification accuracy it is desired to have a small uncertainty interval for a given significance level $\alpha$. But at the present stage of radar development improvement of the influencing radar dependent parameter is very difficult and can only be achieved by the means of expensive hardware improvement. Contrary, a significant development potential for confidence interval shrinkage can be achieved by accurate ego-velocity information. As shown in [5], the velocity provided by the vehicle manufacturer is not always unbiased and can continue to increase as a result of mechanical wear of the involved parts over the life of the vehicle. According to european traffic law, the estimated velocity of a car must not fall below the actual velocity or exceed it by $10\%$ and additional $4\,\mathrm{km\,h^{-1}}$ [7]. If this systematic error in velocity estimate can not be corrected, it must be taken into account via an increased velocity variance. It is important to note, that if the systematic error in ego-velocity increases and will not be compensated or respected in the standard deviation, the classification accuracy will decrease massively since the interval will be biased as well.

To illustrate the effect of uncertainty in ego-velocity with respect to the classification, we compute the angle interval in which a parallel slowly moving target of $v_{\text{obj.}} = 5\,\mathrm{km\,h^{-1}}$ — could be a pedestrian as a common target — will be classified correctly rather then being classified as a stationary target. Therefore the term $\mu_E$, which is basically zero for every stationary target, will shift to $-v_{\text{obj.}}\cos(\mu_\Phi)$ as the difference radial velocity with $\mu_\Phi$ being the angle of arrival, see Figure 2. Now solving for $\mu_\Phi$ gives the angle interval in which the moving target will be classified correctly as dynamic.

$$|\mu_\Phi| \leq \arctan\left(\sqrt{\frac{D}{\mu^2_{V_{\text{Ego}}}\sigma^2_\Phi + \sigma^2_\Phi\sigma^2_{V_{\text{Ego}}}}}\right) \tag{2}$$

with $D$ being

$$D = \left(\frac{v_{\text{obj.}}}{Q^{-1}(\alpha/2)}\right)^2 - \left(\frac{\mu^2_{V_{\text{Ego}}} + \sigma^2_{V_{\text{Ego}}}}{2}\sigma^4_\Phi + (1 - \frac{\sigma^2_\Phi}{2})^2\sigma^2_{V_{\text{Ego}}}\right). \tag{3}$$

This correct classification area is plotted assuming $\sigma_\Phi = 1°$ and $\sigma_{V_{\text{Ego}}} \in \{0, 2, 2.9\}\mathrm{km\,h^{-1}}$ over an ego-velocity spectrum in Figure 1.

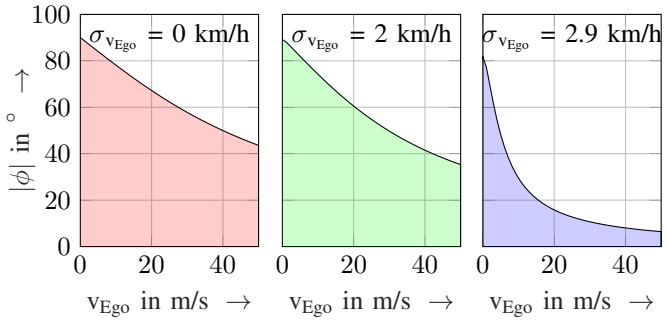


Fig. 1. Angle-Interval in which a slowly parallel moving object is classified correctly versus ego-velocity for $\sigma_{v_{\text{Ego}}} \in \{0, 2, 2.9\}\mathrm{km\,h^{-1}}$

Here one can see, that the dynamic target will be classified correctly at an ego-velocity of $15\,\mathrm{m\,s^{-1}}$ within a angle interval of about $\pm 73°$ for $\sigma_{v_{\text{Ego}}} = 0\,\mathrm{km\,h^{-1}}$. In contrast, if uncertainty of the ego-velocity increases to $\sigma_{v_{\text{Ego}}} = 2\,\mathrm{km\,h^{-1}}$, the interval decreases to $\pm 67°$. An even worse velocity variance, will decrease the angle interval even further as can be seen on the right.

So in order to achieve better classification rates it is necessary to reduce the uncertainty of the ego-velocity. In this section we present method to estimate the ego-velocity based on radar reflections and use this estimate to improve better classification of stationary and dynamic targets.

### *B. Velocity Estimation Based on Stationary Targets*

As described in [6], assuming a stationary target and a longitudinal movement of the ego-vehicle, one can describe the kinematic states as relative values. The radar coordinate system $S$ as well as a stationary point target with qualitative and quantitative relative velocity vector corresponding to longitudinal ego motion are shown in Figure 2.

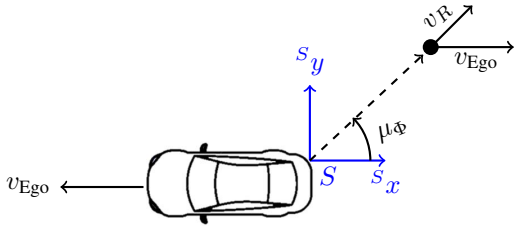


Fig. 2. Transformation from ego-velocity to relative velocity for a stationary point target

Here the radial velocity $v_R$ of a target can be measured by the radar sensor. The velocity information $v_{\text{Ego}}$ of the ego-vehicle can be obtained by the vehicles odometry system. The equation of velocity is then fully described by

$$v_R = v_{\text{Ego}} \cdot \cos(\mu_\Phi). \tag{4}$$

On the set of raw targets, one can estimate the ego-velocity using maximum likelihood estimation methods. In [1], the variance of the radially measured velocities $\sigma^2_{V_r}$ and the variance of the angle measurement $\sigma^2_\Phi$ were modeled as Gaussian distributed and a regression was performed. The Orthogonal Distance Regression (ODR) identifies the regression line through the batch of measurements taking into account the individual variances of the radial-velocity and angle measurements. Due to the non-linearity in (4) and the modeling of the variances in the linear space, the regression line needs to be calculated iteratively. Fortunately the variances are small compared to the correlation due to the coupling from (4). To illustrate this, we simulate multiple realizations of stationary targets and also plot error ellipsoids at discrete points in Figure 3.

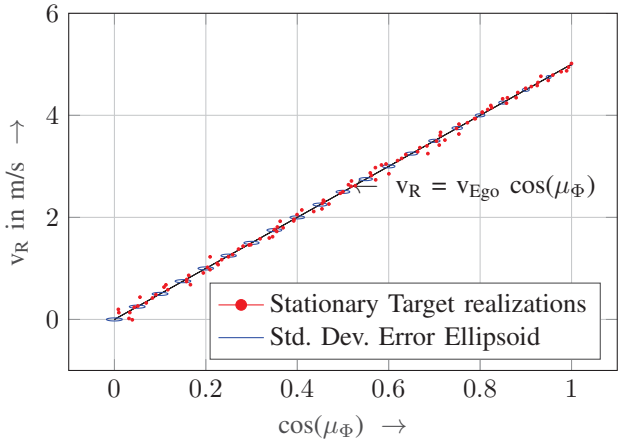


Fig. 3. Functional relationship of $v_R$ and $\cos(\mu_\Phi)$ for stationary targets, error ellipses for stationary targets with $\sigma_\Phi = 1°$, $\sigma_{v_R} = 0.1\,\text{m}\,\text{s}^{-1}$ and $v_{\text{Ego}} = 5\,\text{m}\,\text{s}^{-1}$ (blue) and some realizations (red)

After linearizing with $\cos(\Phi)$ the variances will turn out heteroscedastic, theoretically prohibiting the usage of efficient homoscedastic/linear ODR regression algorithms. Integrated via Principle Component Analysis (PCA) [8] this performs a unitary transformation which maximizes/minimizes the variance for the data

$$z^T = \left[\cos(\mu_\Phi), v_R\right] \tag{5}$$

The velocity estimate is than given by the slope maximizing variance orientation. Since the PCA is performed on the second order moment matrix, the case where poor velocity estimation will occur is, when the second order moments will be dominated by the individual variances $\hat{\sigma}^2_\Phi$ and $\sigma^2_{v_R}$ over the correlating relationship in Figure 3. Assuming one single cluster of targets at $\cos(\mu_\Phi)$ and $v_R = v_{\text{Ego}}\cos(\mu_\Phi)$ the second order moment matrix can be expressed as follows

$$E\left[z \cdot z^T\right] = \underbrace{\begin{bmatrix} \cos(\mu_\Phi)^2 & \cos(\mu_\Phi)^2 v_{\text{Ego}} \\ \cos(\mu_\Phi)^2 v_{\text{Ego}} & \cos(\mu_\Phi)^2 v^2_{\text{Ego}} \end{bmatrix}}_{\text{correlating relationship}} + \underbrace{\begin{bmatrix} \hat{\sigma}^2_\Phi & 0 \\ 0 & \sigma^2_{v_r} \end{bmatrix}}_{\text{error covariance}}. \tag{6}$$

Now considering also a second order matrix, where the disturbing variances are absent, describing perfect measurements, we can compute the error in velocity estimate as the difference between the velocity estimate $\hat{v}_{\text{Ego}}$ from the disturbed second order matrix and the velocity estimate $\tilde{v}_{\text{Ego}}$ from the noise free second order matrix. This error $\nu$ also implies the error due to neglecting heteroscedastic variances. Of interest now is the position interval of the target cluster, at which the velocity estimate falls below a desired error margin, which is here chosen as $\nu = 0.1\,\text{km}\,\text{h}^{-1}$

$$|\tilde{v}_{\text{Ego}} - \hat{v}_{\text{Ego}}| \leq \nu. \tag{7}$$

The velocity estimate for each second order matrix can be computed as the slope of the biggest eigenvector from the corresponding data matrix. This however must be solved numerical giving the interval plotted in Figure 4.

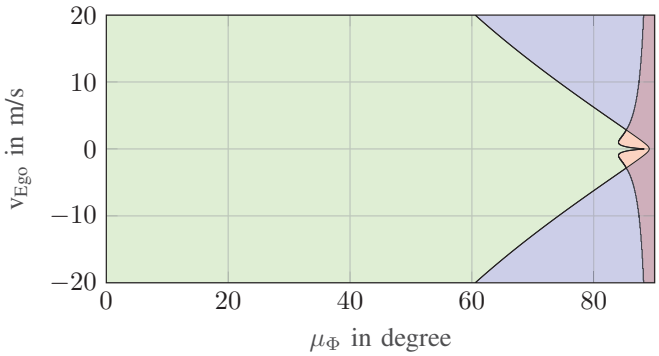


Fig. 4. Angle-Interval at which the estimated velocity differs from the true velocity at more than $\nu = 0.1\,\text{km}\,\text{h}^{-1}$, $\sigma_\Phi = 1°$, $\sigma_{v_r} = 0.03\,\text{m}\,\text{s}^{-1}$ (red). For reference the angle interval from a parallel moving pedestrian would not be classified correctly (blue)

The red area in the figure marks the region, where the difference in true velocity and PCA based velocity estimation exceeds the allowed error interval, so representing the error due to decorrelating noise. The blue marked area describes the region, where the slowly parallel moving target will be misclassified as stationary target thus degrading the velocity estimation (similar to Figure 2). Lastly the green marked area describes the trustworthy region for the velocity estimation. One can clearly see that main degradation is due to possible misclassification instead of decorrelating noise. Since we assume homoscedastic model for velocity estimation but not in the data, this also implies the maximum error due to neglecting the heteroscedasticity. Erroneous velocity estimation due to PCA will appear only if exclusively radar targets oriented

perpendicular to the velocity vector will be observed. This however does not imply, that this will not also take place by using the iterative approach and searching for the optimal solution, since here the decorrelation will also dominate the data structure. And due to the fact, that the distance of the data points to the origin has quadratic influence to second order moment (in mechanical engineering this is called „parallel axes theorem“) stationary targets with high distance to the origin will certainly dominate the calculation of the principle axis. And since $\hat{\sigma}^2_\Phi$ tends towards zero at rising $\cos(\mu_\Phi)$, these targets will not only dominate the principle axis computation but will also lead to improved estimate, telling us, that as long as stationary targets at low $\mu_\Phi$ will be observed, the velocity estimate via PCA is trustworthy.

After computing the binary area, in which the principle components will be dominated by the correlating coupling of (4), it is necessary to compute the error in estimate in order to provide a subsequent Kalman filter proper measurement knowledge. Neglecting heteroscedasticity this can be approximated according to [9] as

$$\hat{\sigma}^2_{v_{\text{Ego}}} \approx \frac{N\lambda_2 \sum_i^N \cos(\phi)_i^2}{(N-1)\left(-\lambda_2 + \sum_i^N \cos(\phi)_i^2\right)^2}. \tag{8}$$

With $\lambda$ being the smaller eigenvalue of the second order moment data matrix and $N$ the number of data points. This represents the variance of the estimate with respect to orthogonal distance, whereas in [1] an variance estimation for orthogonal to axis was given, resulting in a smaller variance estimation. To achieve the best possible velocity estimation, we only utilize radar targets observed within the green marked area from Figure 4 thus to be certain that the radar target stems from a stationary object.

### C. Kalman Filtering the Ego-Velocity Estimate

Since the velocity is crucial for correct classification of stationary targets, it is useful to ensure plausibility via proper model filtering. For this task a common tool is the Kalman filter, which allows the estimation and smoothing of the ego-velocity by means of the modeling the physical transmission behavior of the vehicle in the event of noisy and temporarily missing state measurements [10]. In this section, we model a Kalman filter, taking into account statistical system characteristics that further improve the performance of the speed estimation of the ego-vehicle and the discrimmination of stationary and dynamically moving targets.

Here, a linear transmission behavior with a constant vehicle acceleration is assumed. But since the model assumption of constant acceleration is not suitable for general dynamic driver maneuvers, these modeling errors are taken into account via the system covariance matrix $Q$. For this purpose, an error of the acceleration $\dot{v}_{\text{Ego}_{\text{Error}}}$ is assumed as an additive and average-free normal distributed random variable with variance $\sigma_a^2$ for the constant acceleration $\dot{v}_{\text{Ego}}$. This random acceleration, like the constant acceleration, is projected into the state vector over the second column of the system matrix.

$$\begin{bmatrix} v_{\text{Ego}} \\ \dot{v}_{\text{Ego}} \end{bmatrix}_p = \begin{bmatrix} 1 & \Delta T \\ 0 & 1 \end{bmatrix} \begin{bmatrix} v_{\text{Ego}} \\ \dot{v}_{\text{Ego}} \end{bmatrix} + \begin{bmatrix} \Delta T \\ 1 \end{bmatrix} \dot{v}_{\text{Ego}_{\text{Error}}}. \tag{9}$$

With the random error acceleration

$$\dot{v}_{\text{Ego}_{\text{Error}}} \sim \mathcal{N}\left(0, \sigma_a^2\right) \tag{10}$$

The process covariance from the second central moment of the prediction is then calculated as a random process

$$Q = \begin{bmatrix} \Delta T^2 & \Delta T \\ \Delta T & 1 \end{bmatrix} \sigma_a^2. \tag{11}$$

Since modern vehicles can reach a maximum acceleration of approximately $a_{\text{max}} = 10\,\text{m}\,\text{s}^{-2}$, these values are selected as the maximum deviation in the acceleration. In an interval width around the three-fold standard deviation around the expected value of a normally distributed random variable, approximately $99.7\%$ probability of all realizations are covered. This probability is sufficient for us and allows us to set the hyperparameter $\sigma_a$

$$\begin{aligned} \sigma_a &= \frac{a_{max}}{3} \\ &= \frac{10\,\text{m}\,\text{s}^{-2}}{3}. \end{aligned} \tag{12}$$

The Kalman filter is thus fed from the radar with the ego-velocity point estimate. In the prediction step the Kalman filter then estimates the actual ego-velocity and the velocity variance, which are then used to classify stationary targets. Subsequently stationary targets are utilized to estimate the ego-velocity and measurement error followed by the correction step of the Kalman filter.

If insufficient stationary raw targets have been detected at a time in order to perform an ego-velocity estimate, a prediction of the missing velocity can still be made via the Kalman filter.

### D. Regression Model Based on Odometric Velocity Estimate

If consecutive prediction steps need to be performed, due to little or none stationary targets, the predicted velocity might significantly deviate from the true velocity and the predicted variance will increase fast, so that dynamic targets might be misclassified as stationary targets, it is effective to estimate the velocity based on a corrected odometric velocity $v_{\text{Ego, CAN}}$. This is corrupted due to errors in tire diameter resulting in a linear proportional error term. Therefore we choose the linear model to correct this issue

$$\hat{v}_{\text{Ego, CAN}} = \beta_1 \cdot v_{\text{Ego, CAN}} + \beta_0. \tag{13}$$

While the tire diameter will change over the vehicles lifespan, it is necessary to adapt the model parameters over time, therefore we choose Recursive Least Square (RLS) approach with forgetting (Forgetting parameter $\coloneqq 0.99$) [11] to estimate the ego-velocity via odometrie based velocity signal. As the reference for computing the error at each time step, the Kalman filtered velocity estimate via radar targets is utilized. As the variance estimate for the velocity, the identified values from [6] is used, but surely depends on the ego-vehicle. When the number ob observed stationary targets is less than 5 (we found this to be a proper selection) and the ego-velocity

exceeds $1.5\,\mathrm{m\,s^{-1}}$, so that the unobservable velocity interval via odometry has no effect, the corrected odometrie velocity estimate $\hat{v}_{\mathrm{Ego,\,CAN}}$ is used as a measurement for the Kalman filter. The flow chart of the whole procedure is plotted in Figure 5.

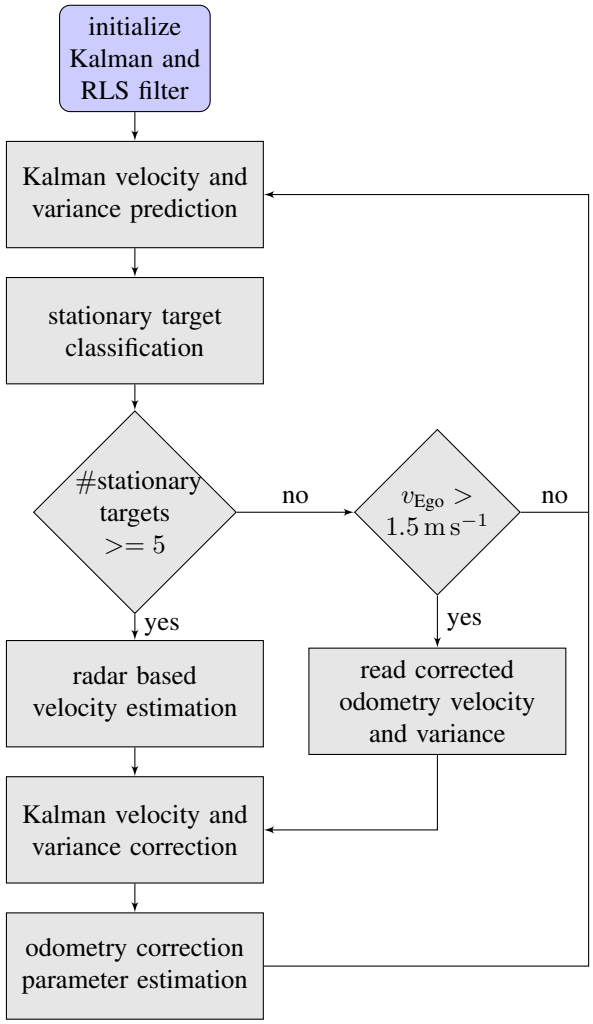


Fig. 5. Flow chart of the proposed algorithm

## III. Results

In order to test the performance of our algorithm, we equipped a test vehicle with a Differential Global Positioning System (DGPS) and a production grade 24 GHz radar sensor mounted at the rear and facing backwards. With this measurement configuration, we carried out a longitudinal dynamic maneuver and recorded the detected raw targets and the velocity of the DGPS system as well as the velocity estimate from vehicles odometry. The results of the different velocity signals for the vehicle under investigation are shown with reference to the DGPS signal for the test run in Figure 6.

It can be observed that the velocity recorded by the CAN differs very strongly from the high-precision DGPS estimate. Just at velocities below $1.5\,\mathrm{m\,s^{-1}}$, the velocity is always

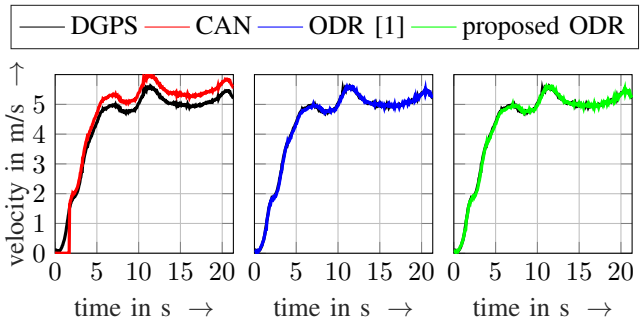


Fig. 6. Ego-velocity over time for DGPS (black), Odometry (red), ODR [1] (blue) and proposed ODR (green) computed ego-velocity signals

measured to $0\,\mathrm{m\,s^{-1}}$. A divergence of the velocity difference is also observable with increasing ego-velocity. In contrast, the ego-velocity estimate of the proposed algorithm as well as the algorithm form [1] deviate only minimal, and no systematic deviation can be determined over the observed velocity spectrum.

To test the performance of the corrected odometric velocity, we synthetically masked out every radar target at time $5\,\mathrm{s} < t < 7\,\mathrm{s}$. It can be seen, that the model produces decent velocity estimate, even the regression model only had a five seconds to initialize itself.

At time $t \geq 14\,\mathrm{s}$ the vehicle passes a parallel moving pedestrian and was able to discriminate it from stationary targets and thus was not infected by defective velocity estimates.

The absence of a systematic measurement error in the velocity is also positively reflected in the classification accuracy of the observed raw targets, see Figure 7.

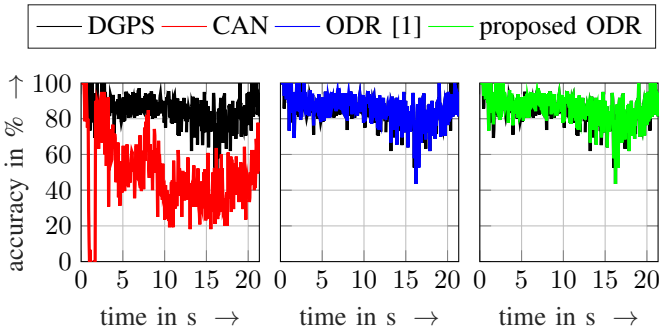


Fig. 7. Classification accuracy for DGPS (black), CAN (red) and Kalman (green) ego-velocity signals

Over the entire scene, the classification accuracy via the radar estimation algorithms achieve performance comparable to that of the DGPS measurement. The classification accuracy of the CAN ego-velocity results in significant losses, which could only be corrected by an increase in the velocity variance. This however would improve the classification accuracy for stationary targets, but at the same time decrease those of moving targets. Precisely in the time interval $1\,\mathrm{s} \leq t < 2\,\mathrm{s}$, the classification accuracy tends to be zero due to the strong

velocity error. For the DGPS system, according to the systems data sheet [12] we choose a standard deviation of $0.05\,\mathrm{km\,h^{-1}}$. For the CAN velocity estimated we choose standard deviation of $0.1\,\mathrm{km\,h^{-1}}$ which was already identified in [6], but not taking into account the velocity dependent systematic error. The standard deviations of the ego-velocity estimations via the radar targets are adaptively estimated via Kalman filter. In Figure 8 we show the estimated standard deviation in ego-velocity used to perform the targets classification. In general

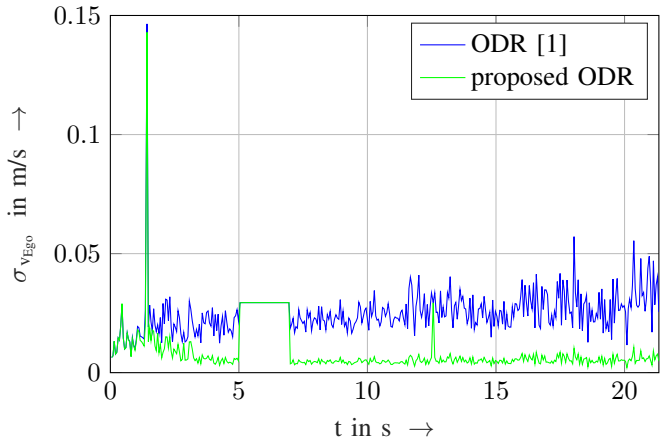


Fig. 8. Standard error of ODR velocity estimation for neglecting heteroscedasticity (green) and respecting heteroscedasticity (blue)

the standard deviation is close to zero, except for a single peak at time $t \approx 1.5\,\mathrm{s}$ where neither a radar target has been in sight nor the ego-velocity exceeds the minimum velocity so that corrected odometry velocity is used. Therefore only Kalman prediction has been performed resulting in a increased variance prediction. Also the fixed standard deviation of $0.1\,\mathrm{km\,h^{-1}} \mathrel{\widehat{=}} 0.0278\,\mathrm{m\,s^{-1}}$ of at time $1.5\,\mathrm{s} \leq t \leq 1.5\,\mathrm{s}$ due to exclusive odometric velocity estimate is observable. Other than that, it can be seen that the proposed algorithm tends to estimate smaller variances compared to the referenced algorithm which arises due to respecting orthogonal variances in its calculation, without significantly effecting accuracy.

## IV. Conclusion

In this paper we have presented an algorithm which is able to successfully estimate the ego-velocity of a vehicle equipped with a radar sensor based on stationary raw targets. This velocity estimation is used in subsequent steps for an improved classification of stationary and moving targets in the radar environment. The classification accuracy was significantly improved even in dynamic driving situations compared to a raw target classification on the odometric based ego-velocity for our specific test vehicle. The general low velocity variance estimate of the proposed algorithm compared to [1] does not translate into significant better accuracy, for which reason the bottleneck for further accuracy improvement is defined mainly by accurate radar angle measurements.

Our algorithm is characterized by a purely forward-directed inference, whereas existing algorithms are iterativley. For an integration on the low computational embedded hardware of series production radar sensors, our algorithm is highly qualified, since it provides assimilable accuracy to the algorithm of [1] but provides low coputational requirements. For a system with $N$ data points and $p$ number of unknown parameters, in general the time complexity of the proposed algorithm via PCA is $\mathcal{O}(\min(p^3, n^3))$ [13] whereas the time complexity of the algorithm from [1] requires the computation of a dense linear system with $\mathcal{O}(p^3)$ for every single iteration [14] also facing more demanding operations (e.g. Jacobian-Matrix). Depending on efficient algorithms and number of iterations for the latter algorithm (set to maximum 10), we found the proposed algorithm on average to run $> 95\%$ faster on our specific computation hardware, even the latter algorithm to exit on average after two iterations due to convergence.

## References


[1] D. Kellner and M. Barjenbruch and K. Dietmayer and J. Klappstein, *Instantanous Lateral Velocity Estimation of a vehicle using doppler radar*, in Proceedings of the 16th International Conference on Information Fusion, 2013.

[2] D. Kellner and M. Barjenbruch and J. Dickmann and K. Dietmayer and J. Klappstein, *Instantanous Ego-Motion Estimation using Doppler Radar*, in Proceedings of the 16th International IEEE Annual Conference on Transportation Systems, 2013.

[3] D. Kellner and M. Barjenbruch and J. Dickmann and K. Dietmayer and J. Klappstein, *Instantanous Ego-Motion Estimation using Multiple Doppler Radars*, in Proceedings of the IEEE International Conference on Robotics & Automation, 2014.

[4] J. Ebbers, *Entwicklung eines Winkelkorrekturverfahrens fuer einen radarbasierten Fahrzeug-Umfeld-Sensor*, B.S. Thesis, Department of Communication Engineering, University of Paderborn, 2014.

[5] M. Rapp and M. Barjenbruch and K. Dietmayer and J. Klappstein and J. DIeckmann, *A fast probabilistic ego-motion estimation framework for radar*, in Proceedings of the IEEE European Conference on Mobile Robots (ECMR), 2015.

[6] C. Grimm and R. Farhoud and T. Fei and E. Warsitz and R. Haeb-Umbach, *Hypothesis test for the detection of moving targets in automotive radar*, (Submitted) in Proceedings of the IEEE International Conference on Microwaves, Communications, Antennas and Electronic Systems, 2017.

[7] Council of European Union, *http://eur-lex.europa.eu/LexUriServ/LexUriServ.do?uri=CELEX:31975L0443:DE:HTML*, Council regulation (EU) no 443/1975.

[8] L. Delchambre, *Weighted principal component analysis: a weighted covariance eigendecomposition approach*, Monthly Notices of the Royal Astronomical Society, Vol. 446, Issue 4, p.3545-3555, 2014.

[9] W. Leyang, *Properties of the total least sqaures estimation*, Geodesy and Geodynamics, Vol. 3, Issue 4, p.39-46, 2012.

[10] R. Kalman, *A new Approach to Linear Filtering and Prediction Problems*, Trans. ASME Journal of Basic Engineering, 1960.

[11] S. Haykin, *Adaptive Filter Theory*, Prentice Hall, Inc., 1996.

[12] GeneSys - Sensor & Navigation Solutions, *ADMA family GPS/Inertial System Automotive/Railway*, https://www.genesys-offenburg.de/en/products/adma-series/, "[Visited; 23. Juni 2017]", 2017.

[13] I. Johnstone and A. Lu, *Sparse Principle Components Analysis*, in the Journal of the American Statistical Association, 2009.

[14] Forth - Institute of computer science, *sparseLM: Sparse Levenberg-Marquardt nonlinear least squares in C/C++*, http://users.ics.forth.gr/~lourakis/sparseLM/, "[Visited; 06. July 2017]", 2017.